ChemPhysChem

Chemistry Europe
European Chemical Societies Publishing

Accepted Article

Title: Towards accurate predictions of proton NMR parameters in molecular solids

Authors: Martin Dracinsky, Jan Vícha, Kateřina Bártová, and Paul Hodgkinson

To be cited as: *ChemPhysChem* 10.1002/cphc.202000629

Link to VoR: https://doi.org/10.1002/cphc.202000629

WILEY-VCH

FULL PAPER WILEY-VCH

Towards accurate predictions of proton NMR parameters in molecular solids

Martin Dračínský,*[a] Jan Vícha,[a,b] Kateřina Bártová[a] and Paul Hodgkinson[c]

[a] Dr. M. Dračínský, K. Bártová
Institute of Organic Chemistry and Biochemistry, AS CR
Flemingovo nám. 2, Prague, CZ-16610, Czech Republic
E-mail: dracinsky@uochb.cas.cz
[b] Dr. J. Vícha
Centre of Polymer Systems
Tomas Bata University in Zlín
Tomáše Bati 5678, Zlín, CZ-760 01, Czech Republic
[b] Prof. P. Hodgkinson
Department of Chemistry,
Durham University, South Road, DH1 3LE, Durham, UK

Supporting information for this article is given via a link at the end of the document.

Abstract: The factors contributing to the accuracy of quantum-chemical calculations of proton NMR chemical shifts in molecular solids are systematically investigated. Proton chemical shifts of six solid amino acids with hydrogen atoms in various bonding environments (CH, CH_2, CH_3, OH, SH and NH_3) were determined experimentally using ultra-fast magic-angle spinning and proton-detected 2D NMR experiments. The standard DFT method commonly used for the calculations of NMR parameters of solids is shown to provide chemical shifts that deviate from experiment by up to 1.5 ppm. The effects of the computational level (hybrid DFT functional, coupled-cluster calculation, inclusion of relativistic spin-orbit coupling) are thoroughly discussed. The effect of molecular dynamics and nuclear quantum effects are investigated using path-integral molecular dynamics (PIMD) simulations. It is demonstrated that the accuracy of the calculated proton chemical shifts is significantly better when these effects are included in the calculations.

Introduction

The number of crystal structures published annually demonstrates the importance of the knowledge of the structure of solids with atomic resolution in many areas of science. The most widely used techniques for determining crystal structures with atomic resolution are diffraction methods. In particular, single crystal X-ray diffraction (XRD) has been called the "gold standard" for solid-state structure determination.[1] Unfortunately, many samples do not provide single crystals of sufficient size and quality for X-ray diffraction.

Solid-state NMR (SS-NMR) spectroscopy is also a powerful and versatile tool for studying the structure and dynamics of solids. SS-NMR experiments do not require long-range order in the studied material and therefore are particularly suitable for powder and amorphous samples. However, complete crystal structures cannot be extracted from experimental NMR data straightforwardly. Therefore, NMR crystallography[2] approaches often compare experimental data with those calculated for a structural model. Most often, density functional theory (DFT) methods are used for the NMR calculations, in particular, the gauge-including projector-augmented wave (GIPAW) procedure was developed for the computations of NMR parameters of fully periodic solids.[3] NMR crystallography in combination with crystal-structure-prediction methods has performed successfully several *de novo* crystal structure determinations.[4] However, NMR crystallography is not limited to ordered crystals; it can provide structural information about disordered or amorphous solids as well.[5] For example, NMR crystallography has been used for investigations of biomolecules adsorbed on surfaces.[6]

It was stressed in many NMR crystallography studies of molecular crystals of organic and pharmaceutically important molecules that chemical shifts of hydrogen atoms are more sensitive to crystal packing than more readily measured carbon chemical shifts.[4a, 4b, 7] Therefore, accurate prediction of hydrogen chemical shifts is essential.

However, quantum chemical calculations of hydrogen chemical shifts may be complicated by nuclear quantum effects (NQEs). Hydrogen atoms possess the lightest nuclei and NQEs, such as nuclear delocalisation or tunnelling may influence properties of hydrogens significantly. Nevertheless, NQEs are normally not included in standard quantum chemical calculations. An elegant and easy way to including NQEs in quantum-chemical simulations is based on the path integral[8] (PI) formalism; the PI equations of motion can be readily coupled with the usual procedures used for molecular dynamics (MD) simulations. We have been developing a methodology for including NQEs in NMR calculations and we demonstrated that including NQEs systematically improves the agreement between calculated and experimental carbon and nitrogen chemical shifts.[9] However, the influence of NQEs on hydrogen chemical shifts of solid materials has not been systematically studied.

The computational level used together with the GIPAW method is currently limited to the general-gradient-approximation (GGA) family of DFT functionals, because periodic plane waves are used as the basis sets, and hybrid density functionals are prohibitively computationally expensive for plane-wave calculations. However, it has been shown in several studies using computations on molecular clusters or fragments of infinite crystals that the use of hybrid density functional or high-level ab initio methods, such as coupled cluster singles and doubles (CCSD), often provides more accurate predictions of NMR parameters of solids.[10] We have recently demonstrated that a simple correction to the GIPAW-GGA result calculated on an isolated molecule at a higher level of theory significantly

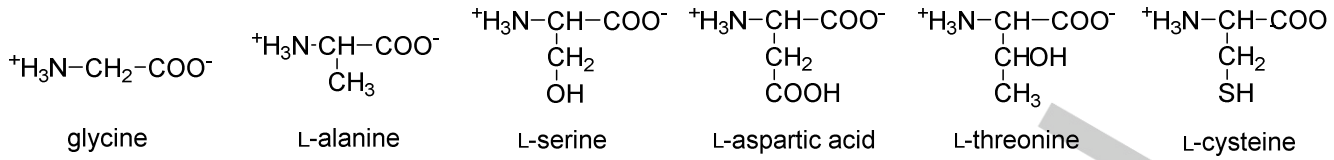

Figure 1. The studied structures.

improves the correlations between experimental and calculated carbon, nitrogen and oxygen chemical shifts.[10f]

Here, we study proton chemical shifts of six solid amino acids (depicted in Figure 1). The selected amino acids have hydrogen atoms in various bonding environments (CH, CH_2, CH_3, OH, SH and NH_3). Experimental high-resolution chemical shifts were newly determined using ultra-fast magic angle spinning (MAS) NMR, and the experimental shifts compared with those calculated at the DFT and coupled-cluster level. The effect of NQEs is investigated using PIMD simulations. The influence of relativistic effects (spin-orbit coupling) on the proton chemical shifts is also discussed.

Results and Discussion

Experiments

Experimental ^{1}H and ^{13}C SS-NMR spectra are shown in the SI together with the proton-detected 2D correlation spectra used for the assignment of the signals. The experimental proton chemical shifts are summarised in Table 1.

In the proton spectrum of L-threonine, the signals of NH_3 protons and of the OH proton are overlapped. To obtain accurate chemical shifts of these two groups, we measured a proton spectrum with a heteronuclear ^{14}N D-HMQC-filter described in refs.[11] where only signals of protons in proximity to a nitrogen atom appear. This spectrum provided the chemical shift of the amino protons and a difference between the standard ^{1}H spectrum and this ^{14}N filtered spectrum provided the chemical shift of the OH group (see details in the SI).

In the proton spectrum of L-serine, there is an unresolved signal of four hydrogens at 3–5 ppm (H-α, H-β and OH). The chemical shift of the OH proton was obtained from a spectrum of partially deuterated L-serine, where all CH hydrogen atoms were labelled with deuterium. The chemical shifts of H-α and H-β were obtained from a 2D CP-INEPT spectrum of fully ^{13}C and ^{2}H-labelled L-serine with the degree of deuteration of ca 97%, which leaves highly diluted ^{13}C-^{1}H spin pairs (Figure S12).

Computations of proton shieldings

Single-point GIPAW calculation of nuclear shieldings for geometry-optimised structures is a standard procedure in most NMR crystallography studies, with a linear fit of the correlation between the calculated shielding and experimental chemical shifts often serving as a measure of the accuracy of the calculations. Furthermore, the parameters of the fitted line are usually used for the referencing and scaling of the chemical shifts, prior to comparison with experiment. The calculated proton shieldings are summarised in Table 1 and the shielding-shift correlation for all investigated hydrogen atoms in this work is shown in Figure 2. The overall correlation is very good, although the SH shielding clearly does not fit well into the linear correlation; its deviation from the fitted line is 1.48 ppm. Three more calculated shieldings deviate from the linear correlation by more than 0.4 ppm (COOH of L-aspartic acid – deviation 0.41 ppm, H-β of L-cysteine – deviation 0.54 ppm and OH of L-serine – deviation 0.66 ppm).

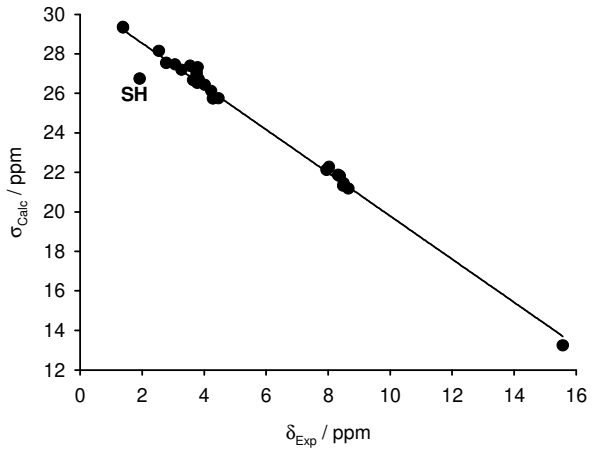

Figure 2. The correlation between calculated ^{1}H shieldings (single-point calculations in CASTEP, geometry optimised structures) and experimental chemical shifts (data from Table 1).

Disorder of the S–H group has been reported in L-cysteine;[12] the thiol group can participate either in S–H···S or in S–H···O hydrogen bonds with a slight preference for the S–H···S arrangement at low temperature.[12c] The number of both molecular arrangements is approximately equal at ambient temperatures (based on analysis of variable-temperature polarised Raman spectroscopy).[12b] We performed geometry optimisation of both crystal structures with the same fixed cell parameters. The structure with the S–H···S hydrogen bond gave a slightly lower energy (by 0.45 kcal/mol per molecule), which corresponds to populations of the two conformers of 68% and 32%, respectively. Accurate predictions of relative energies of crystal structures may require tighter geometry-optimisation criteria,[13] but the exact value of the weighting is not significant here, since both SH calculations show similarly large deviations from the linear shielding-shift correlation. The SH shielding plotted in Figure 2 was calculated as a weighted average of the S–H···S and in S–H···O shieldings with the weighing factor ($x_{S–H···S}$ = 0.68) obtained from the computations. However, changing the weighing factor to $x_{S–H···S}$ = 1 or $x_{S–H···S}$ = 0.5 does not improve the SH shielding with respect to the linear fit with experimental chemical shifts (Figure S18).

Table 1. Experimental ^{1}H chemical shifts, calculated CASTEP shieldings and calculated shielding corrections (ppm). The uncertainty of the experimental chemical shifts was estimated to be ±0.02 ppm. The standard errors of the PIMD corrections estimated as SD/sqrt(*Z*) are given in parentheses.

				Corrections[b]				
	Hydrogen	δ_{Exp}	σ_{Opt}	$\Delta\sigma_{PBE0}$	$\Delta\sigma_{MP2}$	$\Delta\sigma_{CCSD}$	$\Delta\sigma_{SO}$	$\Delta\sigma_{PIMD}$
L-alanine	H-α	3.82	26.71	0.31	0.60	0.76	0.01	–0.65 (0.05)
	NH_3	8.50	21.44	–0.09	–0.10	0.05	0.03	–0.90 (0.07)
	H-β	1.38	29.35	0.08	0.14	0.29	0.01	–0.76 (0.04)
α-glycine	H-α1	4.23	26.12	–0.08	–0.03	0.15	0.04	–0.81 (0.04)
	H-α2	3.06	27.46	0.19	0.43	0.55	0.00	–0.75 (0.03)
	NH_3	8.48	21.32	–0.17	–0.19	–0.04	0.03	–0.57 (0.03)
L-aspartic acid	H-α	3.76	27.04	0.25	0.54	0.70	0.00	–0.85 (0.01)
	NH_3	8.32	21.87	–0.06	–0.08	0.07	0.03	–0.87 (0.00)
	H-β1	3.27	27.19	0.22	0.33	0.59	0.04	–0.86 (0.05)
	H-β2	2.54	28.15	0.04	0.25	0.34	0.00	–0.76 (0.02)
	COOH	15.57	13.24	–0.23	–0.22	0.03	0.06	–0.81 (0.08)
L-threonine	H-α	4.02	26.43	0.18	0.41	0.56	0.01	–0.82 (0.04)
	NH_3	8.03	22.27	–0.06	–0.07	0.10	0.03	–0.65 (0.04)
	H-β	3.78	26.53	0.23	0.36	0.64	0.00	–0.85 (0.03)
	H-γ	1.39	29.33	0.07	0.13	0.29	–0.01	–0.87 (0.02)
	OH	7.95	22.13	–0.12	–0.47	–0.20	0.10	–0.46 (0.04)
L-cysteine[a]	H-α	4.28	25.99	0.31	0.58	0.77	0.03	–0.72 (0.04)
	NH_3	8.65	21.24	–0.10	–0.09	0.06	0.02	–0.63 (0.02)
	H-β1	3.55	27.45	0.23	0.41	0.66	–0.01	–1.03 (0.03)
	H-β2	2.78	27.68	0.23	0.43	0.72	–0.03	–0.93 (0.01)
	SH	1.92	27.01	–0.06	0.00	0.27	0.56	0.55 (0.06)
L-serine	H-α	3.64	26.67	0.31	0.59	0.78	0.02	–0.62 (0.01)
	NH_3	8.37	21.82	–0.07	–0.06	0.10	0.03	–0.73 (0.04)
	H-β1	3.75	26.72	0.33	0.46	0.74	–0.01	–0.80 (0.03)
	H-β2	4.46	25.75	0.20	0.34	0.61	0.00	–0.78 (0.06)
	OH	3.79	27.32	0.03	–0.20	0.10	0.08	–0.78 (0.14)

[a] The S–H···S and S–H···O forms of L-cysteine were taken to be in 0.68:0.32 ratio. [b] Positive corrections indicate higher shielding, i.e. upfield shift.

Isolated-molecule corrections

It has been shown recently that a simple correction of GIPAW shieldings calculated with the hybrid functional PBE0 on an isolated molecule improves the shielding-shift correlations for carbons, nitrogens and oxygens significantly.[10f] The corrections to the amino-acid proton shieldings calculated with the hybrid PBE0 functional ($\Delta\sigma_{PBE0}$) are generally not very large (–0.2 to +0.3 ppm, shown in Table 1); they are positive for all CH, CH_2 and CH_3 hydrogens except for one of the alpha hydrogens in glycine (–0.08 ppm), and negative for all NH_3 protons. The OH and SH corrections are both positive and negative depending on the individual structure. The PBE0 corrections do not, however, improve the shielding-shift correlation; the mean absolute error (MAE), the maximal error (MaxE) and the root mean square deviation (RMSD) are even slightly worse than those obtained for uncorrected GIPAW shieldings (Table 2).

The disorder in L-cysteine gives us an opportunity to investigate whether the calculated corrections are mostly governed by intramolecular effects or by crystal packing. The single-molecule corrections calculated for the two conformers are generally very similar (Table 3). The largest differences are found for the thiol hydrogen, which is probably caused by the slightly shorter S–H bond in the minor conformer (1.357 Å) than in the major conformer (1.365 Å).

We also calculated the molecular corrections at the MP2 and CCSD level ($\Delta\sigma_{MP2}$ and $\Delta\sigma_{CCSD}$). The shielding corrections calculated at MP2 level are generally not far from the PBE0 corrections; the largest difference can be observed for the OH proton in L-threonine, where PBE0 provides a correction of –0.12 ppm and MP2 of –0.47 ppm. All calculated CCSD corrections (shown in Table 2) are systematically 0.1–0.3 ppm higher than MP2 corrections. Note that these computations are extremely demanding and not affordable for larger systems. The CCSD corrections are particularly large (0.55–0.78 ppm) for all alpha hydrogens. However, these MP2 and CCSD corrections did not improve the correlation between experimental and calculated data (Table 2).

We used the 6-311+G(2d,p) basis set for the calculations of molecular corrections because excellent results were obtained previously with this basis set for carbon chemical shifts. Furthermore, it was observed that the basis-set choice has relatively small effect on the calculated molecular corrections of ^{13}C, ^{15}N and ^{17}O shifts.[10f] In order to check whether the choice of the basis set plays an important role in the calculations of proton shieldings, we recalculated the MP2 corrections for glycine, L-alanine and L-serine with aug-ccPVDZ and aug-ccPVTZ basis sets. The corrections calculated with the triple-zeta set was very close to those obtained with 6-311+G(2d,p) set (see Table S1 in the SI).

Table 2. The parameters of the correlation between experimental ^1H shifts and shieldings calculated for geometry-optimised structures and with the isolated-molecule and PIMD corrections. All values apart from the slope are in ppm.

Correction	Slope[a]	Intercept	MAE	MaxE[b]	RMSD
–	–1.10	30.75	0.22	1.49 (SH)	0.37
$\Delta\sigma_{PBE0}$	–1.14	31.07	0.22	1.71 (SH)	0.40
$\Delta\sigma_{MP2}$	–1.16	31.27	0.26	1.76 (SH)	0.42
$\Delta\sigma_{CCSD}$	–1.16	31.47	0.26	1.70 (SH)	0.41
$\Delta\sigma_{SO}$	–1.10	30.85	0.19	1.06 (SH)	0.30
$\Delta\sigma_{PIMD}$	–1.11	30.11	0.18	0.56 (OH)	0.22
$\Delta\sigma_{SO}+\Delta\sigma_{PIMD}$	–1.11	30.17	0.17	0.59 (OH)	0.22
$\Delta\sigma_{PBE0}+\Delta\sigma_{SO}+\Delta\sigma_{PIMD}$	–1.14	30.43	0.17	0.48 (OH)	0.21
$\Delta\sigma_{CCSD}+\Delta\sigma_{SO}+\Delta\sigma_{PIMD}$	–1.17	30.84	0.17	0.41 (H-α)	0.21

[a] Standard error of the fitted slope is 0.02–0.03 in all cases. [b] The hydrogen atom with maximal error in parenthesis – SH in L-cysteine, OH in L-serine or H-α in L-alanine.

Table 3. The calculated proton shieldings and shielding corrections (in ppm) for the two conformers of L-cysteine. The uncertainty of the experimental chemical shifts was estimated to be ±0.02 ppm. The standard errors of the PIMD corrections estimated as SD/sqrt(*Z*) are given in parentheses.

				Corrections			
	Hydrogen	δ_{Exp}	σ_{Opt}	$\Delta\sigma_{PBE0}$	$\Delta\sigma_{CCSD}$	$\Delta\sigma_{SO}$	$\Delta\sigma_{PIMD}$
S–H···S	H-α	4.28	25.74	0.31	0.77	0.03	–0.76 (0.04)
	NH_3	8.65	21.18	–0.09	0.06	0.02	–0.57 (0.02)
	H-β1	3.55	27.39	0.20	0.61	–0.01	–0.99 (0.04)
	H-β2	2.78	27.54	0.24	0.74	-0.03	–0.89 (0.02)
	SH	1.92	26.74	–0.10	0.21	0.56	0.74 (0.05)
S–H···O	H-α	4.28	26.24	0.32	0.78	0.04	–0.64 (0.04)
	NH_3	8.65	21.38	–0.11	0.05	0.03	–0.76 (0.01)
	H-β1	3.55	27.59	0.28	0.77	–0.02	–1.12 (0.03)
	H-β2	2.78	27.98	0.20	0.67	–0.02	–1.01 (0.01)
	SH	1.92	27.58	0.02	0.41	0.57	0.14 (0.10)

In the presence of heavy nuclei, any attempt to achieve a reasonable agreement between theory and experiment has to consider relativistic effects in the computations.[14] Particularly important is the effect named spin-orbit heavy-atom on the light-atom (SO-HALA) effect, which affects the most common ^1H, ^{13}C, and ^{15}N nuclei and may shift their signals to unexpected chemical-shift ranges.[15] An overview of relativistic theoretical methods to calculate the NMR parameters of molecules with heavy nuclei can be found in recent reviews.[16] It has been shown that relativistic effects cannot be neglected even in the third-row species, such as chlorine[17] or sulfur,[18] when aiming at high precision and good agreement with the experimental data. For instance, even such a light element like sulfur can induce an overall SO-HALA shielding of –8 ppm at the bound ^{13}C nuclei.[19] It has also been demonstrated that the SO-HALA effect can be transmitted through hydrogen bonds.[20]

While scalar-relativistic treatment is included in the CASTEP shielding calculations at the level of the Koelling-Harmon approximation of the Dirac equation,[21] the effect of the SO coupling is not included. Therefore, we calculated SO corrections ($\Delta\sigma_{SO}$) on isolated molecules similarly as other molecular corrections. These SO corrections are very small for all CH and NH_3 protons (the magnitudes smaller than or equal to 0.04 ppm). They are slightly larger for OH protons (0.06–0.10 ppm) and very important for SH protons in L-cytosine (0.56 and 0.57 ppm for S–H···S and in S–H···O structures, respectively). The inclusion of these relativistic corrections in the shielding calculations significantly reduces the maximal error (Table 2).

PIMD corrections

The influence of NQEs on proton chemical shifts was calculated by NMR calculations on snapshots from PIMD simulations. An example of the convergence of the calculated shieldings of L-alanine with respect to the length of the simulation is shown in Figure 3. The fluctuations of the averaged shieldings (averaging over the time of the simulation and over the chemically equivalent positions) are smaller than 0.05 ppm after 6 ps and smaller than 0.01 ppm after 8 ps averaging. The standard errors of the calculated shieldings for chemically equivalent sites, which are used as an estimation of the error of the PIMD correction are smaller than 0.1 ppm after the 10 ps simulations (Table 1) in all cases except the OH proton in L-serine where it is 0.14 ppm.

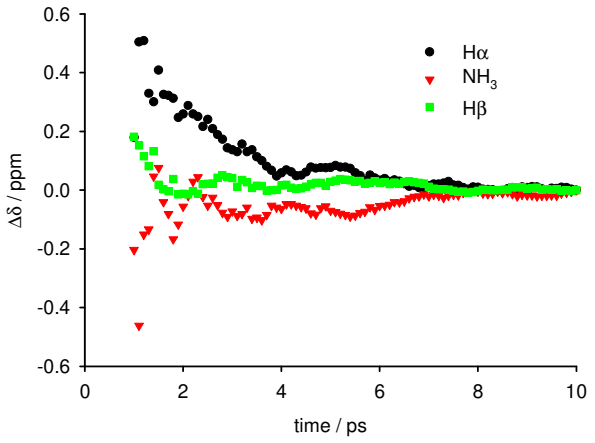

Figure 3. Convergence of the calculated averaged proton chemical shifts of L-alanine with respect to the length of the PIMD simulation (plotted as the difference from the value at t = 10 ps).

The PIMD corrections for protons attached to a carbon are always negative with magnitudes in the range 0.6–1.0 ppm. There is no clear trend for differentiating CH, CH_2 and CH_3 hydrogens. However, the investigated series of compounds is relatively small (e.g. there is only one CH_3 group). Therefore, we also re-examined PIMD simulations performed in our previous work[9a] and analysed the PIMD corrections of methyl-β-D-xylopyranoside, which contains CH, CH_2, CH_3 and OH groups. Also in this compound, the PIMD corrections were similar for all types of hydrogens attached to a carbon (Table S2).

The NH_3 corrections are also always negative and their magnitudes fall in the same range as those of C–H protons. The corrections for the COOH proton of L-aspartic acid and the OH proton of L-serine are close to –0.8 ppm and are thus similar to the corrections for C–H and N–H protons. The magnitude of the correction for the OH proton in L-threonine is slightly smaller (0.46 ppm).

The most interesting PIMD correction is found for the SH proton in L-cysteine, which is the only hydrogen atom in the whole investigated series that provides positive PIMD correction, and the correction is significantly larger for the S–H···S structure (0.74 ppm) than for the S–H···O structure (0.14 ppm).

The agreement with experiment is significantly better when the PIMD corrections are included in the shielding calculations; the maximal error drops to 0.56 ppm (Table 2). However, the best agreement with experiment is obtained when PIMD, SO and CCSD corrections are all added to the shielding calculations; the RMSD value is 0.21, i.e. ca one half of that obtained for GIPAW calculations without any correction and the maximal error is 0.41 ppm (for H-α in L-alanine), i.e. 28 % of the pure-GIPAW value (Table 2, Figure S19). Residual deviations from the linear correlations obtained with pure GIPAW and GIPAW with PIMD, SO and CCSD corrections are shown in Figure 4.

A worrying issue is the slope of the shielding-shift correlation, which is relatively far from the ideal value of –1 in all cases. A possible explanation of this deviation might be a larger error of the isolated point of the COOH hydrogen of L-aspartic acid (experimental δ: 15.57 ppm). Indeed, when this point is omitted from the correlations, the slopes become slightly closer to –1 (from –1.06 to –1.16, Table S3); however, the deviations are still relatively large. Another possible source of error of the slope might be the inaccuracy of the geometry optimisation procedure.[2, 22]

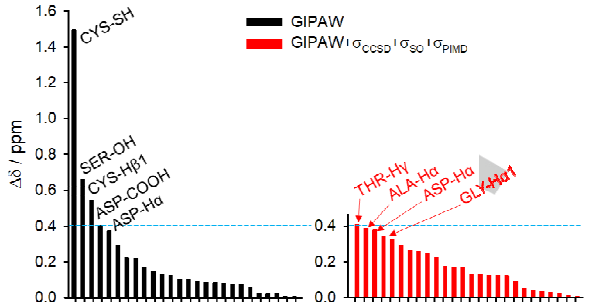

Figure 4. Deviations of individual calculated proton chemical shifts from the linear correlations with experiment ordered by decreasing values (based on the GIPAW calculations). Only deviations larger than 0.3 ppm are assigned to the proton positions. Black bars: GIPAW calculations, red bars: GIPAW calculations with $\Delta\sigma_{CCSD} + \Delta\sigma_{SO} + \Delta\sigma_{PIMD}$ corrections. The deviations were calculated from data presented in Table 1.

Carbon and nitrogen chemical shifts

The calculations of carbon chemical shifts are not the focus of this paper, therefore, they will be discussed only briefly here. Experimental carbon chemical shifts, the calculated shieldings and shielding corrections are shown in Table 4 and the parameters of the linear shielding-shift correlations are shown in Table 5. The carbon shieldings calculated for the geometry optimised structures without any correction correlate reasonably well with the experimental chemical shifts, the MAE is 1.09 ppm and maximal error is 3.21 ppm, which are typical values that can be expected for molecular solids.[10f] Surprisingly, the best improvement of the calculated shieldings is obtained when the very simple and fast PBE0 correction is employed ($\Delta\delta_{PBE0}$ values ranging from –1.4 to 7.6 ppm); the maximal error drops to 1.86 ppm. These calculations thus confirm the previous finding that these corrections calculated with a hybrid density functional improve the accuracy of carbon shieldings significantly.[10f] The SO corrections are less significant; the largest correction of 2.5 ppm is found for the L-cysteine carbon atom directly attached to the sulphur atom, the correction is close to 1.7 ppm for all COO carbons and close to 1 ppm or smaller for all other atoms. Although the magnitude of the SO correction is generally larger for carbon atoms than for hydrogen atoms, the significantly larger range of carbon spectra makes the effect of the SO correction proportionally much smaller. Therefore, the SO correction can probably be safely omitted in most carbon NMR calculations of organic compounds without heavy elements.

Table 4. Experimental ^{13}C chemical shifts, calculated CASTEP shieldings and calculated shielding corrections (ppm). The uncertainty of the experimental chemical shifts was estimated to be ±0.02 ppm. The standard errors of the PIMD corrections estimated as SD/sqrt(*Z*) are given in parentheses.

				Corrections[a]			
	Carbon	δ_{Exp}	σ_{Opt}	$\Delta\sigma_{PBE0}$	$\Delta\sigma_{CCSD}$	$\Delta\sigma_{SO}$	$\Delta\sigma_{PIMD}$
L-alanine	COO	177.71	–9.12	–0.95	7.70	1.68	–1.39 (0.33)
	C-α	50.92	121.27	2.78	10.69	0.24	–5.92 (0.13)
	C-β	20.36	154.11	5.08	13.08	0.87	–5.88 (0.36)
α-glycine	COO	176.25	–7.26	–1.13	7.58	1.71	–2.54 (0.22)
	C-α	43.58	129.82	1.00	7.24	0.15	–5.75 (0.04)
L-aspartic	COO	175.91	–7.20	–0.80	7.75	1.70	–3.25 (0.06)
acid	C-α	53.78	117.15	3.31	11.44	0.27	–4.63 (0.41)
	C-β	37.77	135.49	5.44	14.33	0.59	–6.07 (0.44)
	COOH	174.66	–6.87	–1.10	10.74	1.74	–2.50 (0.33)
L-threonine	COO	172.06	–2.11	–1.38	7.24	1.67	–2.92 (0.22)
	C-α	61.25	110.59	3.40	11.49	0.28	–6.55 (0.33)
	C-β	66.93	101.19	7.11	18.35	1.24	–6.48 (0.37)
	C-γ	20.48	154.54	4.75	12.42	0.80	–6.70 (0.28)
L-cysteine	COO	173.37	–3.77	–1.12	7.50	1.66	–3.12 (0.32)
	C-α	56.01	115.34	2.51	10.12	0.45	–5.74 (0.22)
	C-β	28.09	142.31	6.89	18.02	2.52	–6.34 (0.13)
L-serine	COO	175.05	–5.67	–1.05	7.66	1.66	–1.86 (0.19)
	C-α	55.69	116.16	2.22	9.76	0.39	–4.99 (0.13)
	C-β	62.86	105.52	7.58	18.63	1.14	–5.00 (0.33)

[a] The S–H···S and S–H···O forms of L-cysteine were taken to be in 0.68:0.32 ratio.

Table 5. The parameters of the correlation between experimental ^{13}C shifts and shieldings calculated for geometry-optimised structures and with the isolated-molecule and PIMD corrections. All values except for the slope are in ppm.

Correction	Slope	Intercept	MAE	MaxE[a]	RMSD
–	–1.02	173.05	1.09	3.21 (Tβ)	1.24
δ_{PBE0}	–1.07	179.23	0.87	1.86 (Gα)	0.93
δ_{SO}	–1.02	173.52	1.00	2.91 (Tβ)	1.16
δ_{CCSD}	–1.06	187.62	1.49	4.07 (Gα)	1.61
δ_{PIMD}	–1.00	166.04	1.28	4.48 (Tβ)	1.43
$\delta_{PBE0} + \delta_{SO} + \delta_{PIMD}$	–1.03	172.70	1.26	2.44 (Aβ)	1.23
$\delta_{CCSD} + \delta_{SO} + \delta_{PIMD}$	–1.09	181.10	1.91	4.64 (Gα)	1.96

[a] The carbon atom with maximal error in parenthesis – C-β in L-threonine (Tβ), C-α in glycine (Gα) or C-β in L-alanine (Aβ).

The PIMD corrections are always negative and depend (in agreement with a previous report[9a]) on the number of hydrogen atoms attached to the carbon atom. The magnitudes of the PIMD correction for quaternary carbons are smaller (1.4–3.3 ppm) than for protonated carbon atoms (4.6–6.7 ppm). The fact that the signals of quaternary carbons appear at higher chemical shifts in the ^{13}C NMR spectra than the signals of protonated carbons leads to a change of the slope of the shielding-shift correlation, which has then the ideal value of –1. On the other hand, the inclusion of the PIMD corrections leads to a larger maximal error of 4.5 ppm found for C-β of L-threonine. This larger error may be partially caused by insufficient convergence of the PIMD correction.

Nitrogen chemical shifts of the studied compounds were not determined experimentally. Therefore, only the calculated shieldings and shielding corrections are shown in the SI.

Conclusion

Proton chemical shifts of six solid amino acids were determined using ultra-fast MAS experiments. The selected amino acids have hydrogen atoms in various bonding environments (CH, CH_2, CH_3, OH, SH and NH_3) to cover the most common bonding situations of protons in organic molecules.

The standard DFT method (GIPAW) commonly used for the calculations of NMR parameters of solids is shown to provide chemical shifts with deviations from experiment of up to 1.5 ppm. The largest error was observed for the chemical shift of the SH hydrogen in L-cysteine but the errors were large for several other protons as well.

Corrections to the GIPAW shieldings were calculated for isolated molecules extracted from the geometry-optimised crystal structures. These corrections included a hybrid DFT functional (PBE0), MP2- and CCSD-level calculations and relativistic calculations of spin-orbit coupling. The SO contribution was shown to be very important for hydrogen atoms attached to sulphur. Furthermore, the molecular-dynamics effects and nuclear quantum effects were investigated by PIMD simulations. The corrections obtained from these simulations are similar for all hydrogen atoms attached to a carbon but differ significantly for OH and SH protons involved in intermolecular hydrogen bonding.

The inclusion of the CCSD, SO and PIMD corrections in the NMR chemical shift calculations provides the best agreement with experiment with the RMSD being ca one half of that obtained without any correction. The remaining errors might be ascribed to the GIPAW methodology itself, which was used as the starting point in all calculations, inaccuracies of the DFT, the geometry optimisation protocol and the method for the calculation of corrections for isolated molecules, which neglects many-body effects.

In contrast, the best agreement of carbon chemical shifts with experiment is obtained when the molecular correction calculated with the hybrid PBE0 functional is included in the calculations. This correction can be obtained very fast and with minimal computational cost. This improvement of ^{13}C GIPAW data can probably be ascribed to a fortunate cancellation of errors discussed above.

In summary, this study shows the importance of different sources of errors in calculations of proton, carbon and nitrogen chemical shifts of organic molecular crystals. While hydrogen atoms are very sensitive to nuclear quantum effects captured by PIMD simulations and inclusion of SO-HALA effect is crucial for hydrogen atoms attached to heavier elements, very accurate carbon chemical shifts can be obtained with a simple molecular correction of the DFT functional.

Experimental Section

Samples

Crystalline samples of the studied amino acids were purchased from Sigma-Aldrich. A crystalline sample of isotopically labelled L-serine-1,2,3-$^{13}C_3$-1,2,2-$^{2}H_3$ with the degree of deuteration of ca 97% was obtained from Cambridge Isotope Laboratories, Inc. The sample was further recrystallized from a mixture of D_2O and CH_3CH_2OD to obtain a sample with the ^2H isotope also in the NH_3 and OH groups.

Experiments

High-resolution ^1H and ^{13}C solid-state NMR spectra were obtained using a JEOL ECZ600R spectrometer operating at 43.4 MHz for ^{14}N, 150.9 MHz for ^{13}C and 600.2 MHz for ^1H. Samples were packed into 1 and 3.2 mm magic angle spinning rotors (MAS) and measurements taken at MAS rates of 70 and 18 kHz, respectively. ^{13}C spectra were measured using cross polarization (CP). The chemical shifts were referenced to the signal of sodium trimethylsilylpropanesulfonate (DSS), which was used as an internal standard ($\delta(^1H) = \delta(^{13}C) = 0$). The ramped amplitude shape pulse was used during the cross-polarization. The contact time for CP was 5 ms and the relaxation delays were estimated from ^1H saturation recovery experiments and ranged from 1.5 s for glycine to 50 s for L-aspartic acid. Proton-detected ^1H–^{14}N heteronuclear dipolar recoupling experiments (D-HMQC) were measured at MAS rates of 70 kHz with the $SR4_1^2$ recoupling sequence.[23] These experiments were performed as one-dimensional (i.e. ^{14}N-filtered proton spectra) with the recoupling time of 0.09 ms.[11] The assignment of the signals was done with the help of a 2D inverse HETCOR experiment or 2D CP-INEPT experiment showing C–H correlations via dipolar coupling or J-coupling, respectively. These 2D experiments were taken at MAS rates of 70 kHz and the spectra are shown in the SI. In cases of well-separated signals, proton chemical shifts were obtained by fitting the 1D ^1H signals to a Lorentzian line shape in MestReNova, Version 12.0.1 (Mestrelab Research S.L.). The chemical shifts of overlapping signals in ^1H spectra were obtained from the 2D CP-INEPT spectra. The chemical shifts are reported with two decimal places and the uncertainty is estimated to be ±0.02 ppm.

Structures

Structures of α-glycine, L-threonine, L-aspartic acid, L-cysteine and L-serine determined by X-ray diffraction (XRD) and of L-alanine determined by neutron diffraction (CSD refcodes GLYCIN29, LTHREO01, LASPRT, LCYSTN21, LSERIN01 and LALNIN12) were obtained from the Cambridge Crystallographic Database.[24] All selected crystal structures were determined at room temperature to better match the lattice cell parameters of the crystalline material used for SS-NMR experiments.

NMR shieldings in infinite crystals

The NMR shieldings of the studied structures were calculated by the CASTEP program,[25] version 17.2, which is a DFT-based code that uses pseudopotentials to model the effects of core electrons, and plane waves to describe the valence electrons. Positions of all atoms were optimized prior to the NMR calculation, with fixed unit cell parameters. The geometry optimization is particularly important for XRD structures obtained at r.t. (as those in this study) because molecular dynamics including vibrational and librational motion leads to apparent shrinking of bond distances.[26] No dispersion correction was used as our previous study indicated that these corrections have a negligible effect on calculations of chemical shifts for structures with fixed lattice parameters.[10f, 27] On the other hand, another work has shown that optimising the parameters of dispersion correction can significantly improve predictions of NMR parameters.[28] Electron-correlation effects were modeled using the generalized gradient approximation of Perdew, Burke, and Ernzerhof (PBE).[29] A plane wave basis set energy cutoff of 600 eV, default 'on-the-fly generation' pseudopotentials, and a minimum k-point spacing of 0.05 $Å^{-1}$ over the Brillouin zone via a Monkhorst-Pack grid[30] was used. The NMR calculations were performed using the GIPAW approach.[3a, 31]

PIMD simulations

The PIMD simulations were also performed in CASTEP using an NVT ensemble, temperature of 300 K, Langevin thermostat, 0.5 fs integration time step, ultrasoft pseudopotentials,[32] and planewave cutoff energy of 300 eV. Integrals were taken over the Brillouin zone using a Monkhorst-Pack[30] grid of minimum k-point sampling of 0.1 $Å^{-1}$. Electron-correlation effects were modeled using the PBE functional. The atomic positions were optimized by energy minimization prior to the MD runs at the same computational level. The lattice parameters were fixed to the experimental values. No symmetry constraints were applied during the runs, as these are only relevant to the time-averaged structure. Simulations 10 ps long were performed for every compound. The path integral propagation used a Trotter decomposition of all nuclei into 16 beads, which has been shown to be sufficient for simulations of molecular crystals at 300 K.[9b] The PIMD simulations took 2–8 days on a computational cluster with 16 cores.

PIMD corrections

Time-averaged NMR parameters were computed from 91 snapshots from the PIMD simulations selected at 1.0, 1.1, 1.2 … 10.0 ps. The unit cells of α-glycine, L-alanine, L-threonine, L-cysteine and L-serine contain four crystallographically equivalent molecules (Z = 4), while the unit cell of L-aspartic acid contains two crystallographically equivalent molecules (Z = 2); therefore, 364 or 182 values were averaged for every chemically equivalent site. Since the snapshot values in an individual time series are expected to be significantly correlated, the standard error on the averaged values is estimated as SD/sqrt(Z) where SD is the standard deviation of the values. The PIMD-induced change of isotropic shielding was then calculated as the difference between the averaged NMR parameters and those calculated for the structure optimised at the same computational level used for the PIMD simulations. The NMR calculations took ca 1 day on 160 cores for every amino acid.

Isolated-molecule corrections

DFT NMR shieldings for the isolated molecules (in vacuum) were calculated by the Gaussian16 program.[33] The gas-phase molecule input geometries were taken from the periodic DFT geometry-optimized structures and were not further optimized. PBE and PBE0 functionals together with the 6-311+G(2d,p) basis set were used for the calculations. The PBE0 correction was obtained as the difference between the PBE0 and PBE chemical shieldings.

The calculated corrections using Møller–Plesset perturbation theory to the second order (MP2)[34] with the 6-311+G(2d,p), aug-ccPVDZ and aug-ccPVTZ basis sets were also calculated in Gaussian16.

NMR shieldings at the coupled cluster singles and doubles (CCSD)[35] level and 6-311+g(2d,p) basis set were calculated with the CFOUR program package, which is suitable for performing high-level quantum chemical calculations on atoms and molecules.[36]

Spin-orbit (SO) corrections to NMR chemical shifts were obtained as a difference between scalar relativistic and two-component relativistic (spin-orbit ZORA)[37] shielding calculated at PBE0/TZP level in ADF 2018[38] software package. Contributions of exchange-correlation kernel to SO contribution to NMR shielding were also included.[39]

Acknowledgements

The work was supported by the Czech Science Foundation (grant no. 20-01472S) and by the Ministry of Education, Youth and Sports of the Czech Republic under the National Sustainability Program I (LO1504) to JV.

Keywords: NMR spectroscopy • DFT calculations • solid state • amino acids • molecular dynamics

[1] A. D. Bond, *CrystEngComm* **2012**, *14*, 2363-2366.

[2] P. Hodgkinson, *Prog. Nucl. Magn. Reson. Spectrosc.* **2020**, *118-119*, 10-53.

[3] a) C. J. Pickard, F. Mauri, *Phys. Rev. B* **2001**, *6324*, 245101; b) C. Bonhomme, C. Gervais, F. Babonneau, C. Coelho, F. Pourpoint, T. Azais, S. E. Ashbrook, J. M. Griffin, J. R. Yates, F. Mauri, C. J. Pickard, *Chem. Rev.* **2012**, *112*, 5733-5779; c) S. E. Ashbrook, D. McKay, *Chem. Commun.* **2016**, *52*, 7186-7204; d) T. Charpentier, *Solid State Nucl. Magn. Reson.* **2011**, *40*, 1-20.

[4] a) M. Baias, C. M. Widdifield, J. N. Dumez, H. P. G. Thompson, T. G. Cooper, E. Salager, S. Bassil, R. S. Stein, A. Lesage, G. M. Day, L. Emsley, *Phys. Chem. Chem. Phys.* **2013**, *15*, 8069-8080; b) M. Baias, J. N. Dumez, P. H. Svensson, S. Schantz, G. M. Day, L. Emsley, *J. Am. Chem. Soc.* **2013**, *135*, 17501-17507; c) C. M. Widdifield, H. Robson, P. Hodgkinson, *Chem. Commun.* **2016**, *52*, 6685-6688; d) J. K. Harper, D. M. Grant, *Cryst. Growth Des.* **2006**, *6*, 2315-2321; e) C. M. Widdifield, S. O. N. Lill, A. Broo, M. Lindkvist, A. Pettersen, A. S. Ankarberg, P. Aldred, S. Schantz, L. Emsley, *Phys. Chem. Chem. Phys.* **2017**, *19*, 16650-16661.

[5] a) P. Florian, D. Massiot, *CrystEngComm* **2013**, *15*, 8623-8626; b) M. Dračínský, P. Hodgkinson, *RSC Adv* **2015**, *5*, 12300-12310.

[6] a) E. L. Buckle, J. S. Lum, A. M. Roehrich, R. E. Stote, B. Vandermoon, M. Dracinsky, S. F. Filocamo, G. P. Drobny, *J. Phys. Chem. B* **2018**, *122*, 4708-4718; b) A. Roehrich, G. Drobny, *Acc. Chem. Res.* **2013**, *46*, 2136-2136.

[7] a) E. Salager, G. M. Day, R. S. Stein, C. J. Pickard, B. Elena, L. Emsley, *J. Am. Chem. Soc.* **2010**, *132*, 2564; b) E. Salager, R. S. Stein, C. J. Pickard, B. Elena, L. Emsley, *Phys. Chem. Chem. Phys.* **2009**, *11*, 2610-2621; c) E. A. Engel, A. Anelli, A. Hofstetter, F. Paruzzo, L. Emsley, M. Ceriotti, *Phys. Chem. Chem. Phys.* **2019**, *21*, 23385-23400; d) A. Hofstetter, M. Balodis, F. M. Paruzzo, C. M. Widdifield, G. Steyanato, A. C. Pinon, P. J. Bygrave, G. M. Day, L. Emsley, *J. Am. Chem. Soc.* **2019**, *141*, 16624-16634.

[8] R. P. Feynman, A. R. Hibbs, *Quantum Mechanics and Path Integrals*, McGraw-Hill, New York, **1965**.

[9] a) M. Dračínský, P. Hodgkinson, *Chem. Eur. J.* **2014**, *20*, 2201-2207; b) M. Dračínský, P. Bouř, P. Hodgkinson, *J. Chem. Theory Comput.* **2016**, *12*, 968-973; c) M. Dračínský, L. Čechová, P. Hodgkinson, E. Procházková, Z. Janeba, *Chem. Commun.* **2015**, *51*, 13986-13989; d) K. Bártová, L. Čechová, E. Procházková, O. Socha, Z. Janeba, M. Dračínský, *J. Org. Chem.* **2017**, *82*, 10350-10359.

[10] a) J. D. Hartman, R. A. Kudla, G. M. Day, L. J. Mueller, G. J. O. Beran, *Phys. Chem. Chem. Phys.* **2016**, *18*, 21686-21709; b) J. D. Hartman, G. M. Day, G. J. O. Beran, *Cryst. Growth Des.* **2016**, *16*, 6479-6493; c) J. D. Hartman, A. Balaji, G. J. O. Beran, *J. Chem. Theory Comput.* **2017**, *13*, 6043-6051; d) J. D. Hartman, G. J. O. Beran, *Solid State Nucl. Mag.* **2018**, *96*, 10-18; e) O. Socha, P. Hodgkinson, C. M. Widdifield, J. R. Yates, M. Dračínský, *J. Phys. Chem. A* **2017**, *121*, 4103-4113; f) M. Dračínský, P. Unzueta, G. J. O. Beran, *Phys. Chem. Chem. Phys.* **2019**, *21*, 14992-15000.

[11] a) T. Kobayashi, Y. Nishiyama, M. Pruski, in *Modern Methods in Solid-state NMR - A practitioner's guide* (Ed.: P. Hodgkinson), The Royal Society of Chemistry, Cambridge, **2018**; b) K. Bártová, I. Císařová, A. Lyčka, M. Dračínský, *Dyes Pigments* **2020**, *178*, 108342.

[12] a) K. A. Kerr, J. P. Ashmore, T. F. Koetzle, *Acta Cryst. B* **1975**, *31*, 2022-2026; b) B. A. Kolesov, V. S. Minkov, E. V. Boldyreva, T. N. Drebushchak, *J. Phys. Chem. B* **2008**, *112*, 12827-12839; c) S. A. Moggach, S. J. Clark, S. Parsons, *Acta Crystallogr E* **2005**, *61*, O2739-O2742.

[13] H. E. Kerr, H. E. Mason, H. A. Sparkes, P. Hodgkinson, *CrystEngComm* **2016**, *18*, 6700-6707.

[14] J. Autschbach, T. Ziegler, in *Encyclopedia of NMR* (Ed.: R. K. Harris), John Wiley & Sons, Ltd, Chichester, **2012**.

[15] a) A. H. Greif, P. Hrobárik, J. Autschbach, M. Kaupp, *Phys. Chem. Chem. Phys.* **2016**, *18*, 30462-30474; b) L. A. Seaman, P. Hrobárik, M. F. Schettini, S. Fortier, M. Kaupp, T. W. Hayton, *Angew. Chem. Int. Ed.* **2013**, *52*, 3259-3263; c) P. Hrobarik, V. Hrobarikova, A. H. Greif, M. Kaupp, *Angew. Chem. Int. Ed.* **2012**, *51*, 10884-10888; d) J. Vícha, R. Marek, M. Straka, *Inorg. Chem.* **2016**, *55*, 1770-1781; e) J. Vícha, R. Marek, M. Straka, *Inorg. Chem.* **2016**, *55*, 10302-10309.

[16] a) J. Autschbach, S. Zheng, *Annu. Rep. NMR Spectrosc.* **2009**, *67*, 1-95; b) J. Vícha, J. Novotný, S. Komorovsky, M. Straka, M. Kaupp, R. Marek, *Chem. Rev.* **2020**, *in press*, DOI: 10.1021/acs.chemrev.9b00785; c) M. Kaupp, in *Theoretical and Computational Chemistry* (Ed.: P. Schwerdtfeger), Elsevier, **2004**, pp. 552-597.

[17] S. Standara, K. Maliňáková, R. Marek, J. Marek, M. Hocek, J. Vaara, M. Straka, *Phys. Chem. Chem. Phys.* **2010**, *12*, 5126-5139.

[18] P. Lantto, J. Vaara, A. M. Kantola, V. V. Telkki, B. Schimmelpfennig, K. Ruud, J. Jokisaari, *J. Am. Chem. Soc.* **2002**, *124*, 2762-2771.

[19] Y. Y. Rusakov, I. L. Rusakova, *Magn. Reson. Chem.* **2018**, *56*, 716-726.

[20] J. Vícha, P. Švec, Z. Růžičková, M. A. Samsonov, K. Bártová, A. Růžička, M. Straka, M. Dračínský, *Chem. Eur. J.* **2020**, *26*, 8698-8702.

[21] D. D. Koelling, B. N. Harmon, *J. Phys. C Solid St. Phys.* **1977**, *10*, 3107-3114.

[22] Ł. Szeleszczuk, D. M. Pisklak, M. Zielińska-Pisklak, *J. Comput. Chem.* **2018**, *39*, 853-861.

[23] A. Brinkmann, A. P. M. Kentgens, *J. Am. Chem. Soc.* **2006**, *128*, 14758-14759.

[24] F. H. Allen, *Acta Cryst. B* **2002**, *58*, 380-388.

[25] S. J. Clark, M. D. Segall, C. J. Pickard, P. J. Hasnip, M. J. Probert, K. Refson, M. C. Payne, *Z. Kristallogr.* **2005**, *220*, 567-570.

[26] M. Dračínský, P. Hodgkinson, *CrystEngComm* **2013**, *15*, 8705-8712.

[27] J. Vícha, M. Patzschke, R. Marek, *Phys. Chem. Chem. Phys.* **2013**, *15*, 7740-7754.

[28] a) S. T. Holmes, R. J. Iuliucci, K. T. Mueller, C. Dybowski, *J. Chem. Phys.* **2017**, *146*; b) S. T. Holmes, R. W. Schurko, *J. Phys. Chem. C* **2018**, *122*, 1809-1820.

[29] J. P. Perdew, K. Burke, M. Ernzerhof, *Phys. Rev. Lett.* **1996**, *77*, 3865-3868.

[30] H. J. Monkhorst, J. D. Pack, *Phys. Rev. B* **1976**, *13*, 5188-5192.

[31] J. R. Yates, C. J. Pickard, F. Mauri, *Phys. Rev. B* **2007**, *76*, 024401.

[32] D. Vanderbilt, *Phys. Rev. B* **1990**, *41*, 7892-7895.

[33] M. J. Frisch, G. W. Trucks, H. B. Schlegel, G. E. Scuseria, M. A. Robb, J. R. Cheeseman, G. Scalmani, V. Barone, G. A. Petersson, H. Nakatsuji, X. Li, X. Caricato, A. V. Marenich, J. Bloino, B. G. Janesko, R. Gomperts, B. Mennucci, H. P. Hratchian, J. V. Ortiz, A. F. Izmaylov, J. L. Sonnenberg, D. Williams-Young, F. Ding, F. Lipparini, F. Egidi, J. Goings, B. Peng, A. Petrone, T. Henderson, D. Ranasinghe, V. G. Zakrzewski, J. Gao, N. Rega, G. Zheng, W. Liang, M. Hada, M. Ehara, K. Toyota, R. Fukuda, J. Hasegawa, M. Ishida, T. Nakajima, Y. Honda, O. Kitao, H. Nakai, T. Vreven, K. Throssell, J. Montgomery, J. A. , J. E. Peralta, F. Ogliaro, M. J. Bearpark, J. J. Heyd, E. N. Brothers, K. N. Kudin, V. N. Staroverov, T. A. Keith, R. Kobayashi, J. Normand, K. Raghavachari, A. P. Rendell, J. C. Burant, S. S. Iyengar, J. Tomasi, M. Cossi, J. M. Millam, M. Klene, C. Adamo, R. Cammi, J. W. Ochterski, R. L. Martin, K. Morokuma, O. Farkas, J. B. Foresman, D. J. Fox, Gaussian, Inc., Wallingford CT, **2016**.

[34] C. Møller, M. S. Plesset, *Phys Rev* **1934**, *46*, 618-622.

[35] a) R. J. Bartlett, G. D. Purvis, *Int. J. Quantum Chem.* **1978**, *14*, 561-581; b) J. Čížek, in *Advances in Chemical Physics, Volume 14* (Eds.: R. LeFebvre, C. Moser), John Wiley & Sons, Ltd., London, **1969**, pp. 35-89; c) G. D. Purvis, R. J. Bartlett, *J. Chem. Phys.* **1982**, *76*, 1910-1918; d) G. E. Scuseria, C. L. Janssen, H. F. Schaefer, *J. Chem. Phys.* **1988**, *89*, 7382-7387.

[36] a) A. A. Auer, J. Gauss, *J. Chem. Phys.* **2001**, *115*, 1619-1622; b) CFOUR, Coupled-Cluster techniques for Computational Chemistry, a quantum-chemical program package by J.F. Stanton, J. Gauss, L. Cheng, M.E. Harding, D.A. Matthews, P.G. Szalay with contributions from A.A. Auer, R.J. Bartlett, U. Benedikt, C. Berger, D.E. Bernholdt, Y.J. Bomble, O. Christiansen, F. Engel, R. Faber, M. Heckert, O. Heun, M. Hilgenberg, C. Huber, T.-C. Jagau, D. Jonsson, J. Jusélius, T. Kirsch, K. Klein, W.J. Lauderdale, F. Lipparini, T. Metzroth, L.A. Mück, D.P. O'Neill, D.R. Price, E. Prochnow, C. Puzzarini, K. Ruud, F. Schiffmann, W. Schwalbach, C. Simmons, S. Stopkowicz, A. Tajti, J. Vázquez, F. Wang, J.D. Watts and the

integral packages MOLECULE (J. Almlöf and P.R. Taylor), PROPS (P.R. Taylor), ABACUS (T. Helgaker, H.J. Aa. Jensen, P. Jørgensen, and J. Olsen), and ECP routines by A. V. Mitin and C. van Wüllen. For the current version, see http://www.cfour.de.

[37] a) E. van Lenthe, E. J. Baerends, J. G. Snijders, *J. Chem. Phys.* **1994**, *101*, 9783-9792; b) E. van Lenthe, E. J. Baerends, J. G. Snijders, *J. Chem. Phys.* **1993**, *99*, 4597-4610.

[38] S. ADF 2018, Theoretical Chemistry, Vrije Universiteit, Amsterdam, The Netherlands, http://sww.scm.com.

[39] a) J. Autschbach, *Mol. Phys.* **2013**, *111*, 2544-2554; b) J. Vicha, J. Novotny, M. Straka, M. Repisky, K. Ruud, S. Komorovsky, R. Marek, *Phys. Chem. Chem. Phys.* **2015**, *17*, 24944-24955.

Entry for the Table of Contents

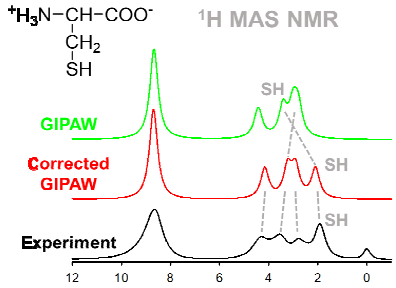

The factors contributing to the accuracy of quantum-chemical calculations of proton NMR chemical shifts in molecular solids are systematically investigated. The effects of the computational level (hybrid DFT functional, coupled-cluster calculation, inclusion of relativistic spin-orbit coupling) and nuclear quantum effects are thoroughly discussed and a method for accurate chemical-shift prediction is proposed.

Institute and/or researcher Twitter usernames: @IOCBPrague